ORIGINAL PAPER

Effect of biofilm on naval steel corrosion in natural seawater

**Souad Belkaid · Mohamed Arezki Ladjouzi ·
Samir Hamdani**

Abstract The behaviour of steel in natural environments is
not only dependent on material properties and environmen-
tal aggressiveness, but also on micro-organisms which can
exist within it. The electrochemical evolution of the
interface formed on BV-grade A naval steel exposed to
natural seawater in the presence and absence of marine
micro-organisms has been studied over 30 days. The results
obtained by electrochemical techniques including linear
polarisation and electrochemical impedance spectroscopy
revealed that a heterogeneous layer formed by a mixture of
corrosion products and biofilm grew on the material surface
in natural seawater, producing an increase of the corrosion
rate and then a decrease in the corrosion resistance under
diffusion process. In this case, the protective layer formed
by the corrosion products can be subject to the localised
breakdown. In sterile seawater, the formation of two layers
at the metal surface generated by organic and/or inorganic
compounds deposits (outer layer) and corrosion products
(inner layer) is concluded. Using our experimental data,
electrical models are proposed. They describe the imped-
ance distribution for carbon steel exposed to both environ-
ments. Scanning electron microscopy, energy dispersive
X-ray spectrometry analysis and optic microscope repro-
ductions were obtained. They allowed an interpretation of
the effect of the marine biofilm on the behaviour of the
carbon steel in seawater.

S. Belkaid (✉) · M. A. Ladjouzi
Laboratoire d'Electrochimie-Corrosion, Métallurgie et Chimie
minérale, Université des sciences et de technologies Houari
Boumediene (USTHB),
BP 32 El Alia, Bab Ezzouar 16111, Alger, Algérie
e-mail: belkaid_so@yahoo.fr

S. Hamdani
Laboratoire des systèmes électriques et industriels, Université des
sciences et de technologies Houari Boumediene (USTHB),
BP 32 El Alia, Bab Ezzouar 16111, Alger, Algérie

Introduction

Microbiologically influenced corrosion (MIC) has been
studied since the beginning of the twentieth century as
reported by some authors [1, 2]. This phenomenon is
responsible for the degradation of many metallic structures
[3, 4]. Generally, MIC occurs simultaneously with the
appearance of a biofilm with gelatinous aspect. The biofilm
is the sessile bacterial population growing on surfaces, and
frequently embedded in a matrix of extracellular polymeric
substances [5]. A population of bacterial cells may include
cells of either one or many species: the aerobic bacteria
create a gradient of oxygen by their breath inside the
biofilm. In entirely oxygen-free zones, the anaerobic strains
can be found and participate both with the aerobic bacteria,
to the increase of the corrosion.

In seawater, the biofilm can be formed within few hours
[6]. Indeed, this medium is rich with various nourishing
elements such as carbon, sulphur, calcium and magnesium
which constitute a source of energy. These elements are
necessary for the enzymatic activities and have a catalytic
role in the bacterial cell. Generally, bacterial populations in
marine biofilms formed on the surface of steel have a
heterogeneous nature: aerobic bacteria, anaerobic bacteria
and mushrooms. Microbial corrosion induced by some
sulphate reducing bacteria (SRB) strains is mainly due to
the catalysis of a cathodic reduction of proton (or water) by
formation of ferrous sulphides [7]. These biofilms covering
steel can also contain dissimilatory iron-reducing bacteria
because the solid ferric oxides are good electron acceptors
for them [8]. Aerobic *Pseudomonas* strains, most prevalent
in seawater, have been found being involved in the

corrosion of mild steel [9, 10]. The bacterial activities on iron and steel can alter the oxides structures that form the passive layer by increasing their dissolution and removing them from the metal surface which tends to promote the initiation then the propagation of pitting corrosion [11, 12].

Extensive investigations have been carried out to determine the composition of the products formed at the surface of carbon steel immersed in seawater. Duan et al. [13, 14] reported that the rust is composed of three layers: outer, middle and inner. The presence of goethite (α-FeOOH) and lepidocrocite (γ-FeOOH) iron oxides into outer and middle layers, of brown and yellow colour, respectively, have been confirmed by scanning electron microscopy (SEM) and XRD analysis. The main compound in the inner layer is a mixture of hydroxy sulphate and siderite ($FeCO_3$) with attached bacteria. Also, the presence of pyrite FeS_2 and mackinawite (FeS) associated to the SRB is detected at the surface of materials immersed in seawater [15, 16]. On the other hand, Sosa et al. [17] revealed that two layers are formed when carbon steel is exposed to natural seawater. The outer layer is due to chemical precipitation of the species present in seawater or biofilm influence. In the inner layer, the iron oxide is the predominant compound.

In this paper, the influence of a marine biofilm on the carbon steel/seawater interface has been studied under laboratory conditions using the impedance measurement. This technique is powerful for the characterisation of the electrochemical behaviour of carbon steel when a biofilm may form in natural environments containing micro-organisms. It gives further knowledge of the interface physical characteristics such as capacitance and metallic resistance. The interfacial evolution along time has been analysed too. This study is completed by linear polarisation measurements and SEM observations of the surface.

Experiments

The naval carbon steel BV-grade A has been investigated in this study. This sample is widely used for offshore building. Its nominal elemental composition (wt) was: Fe 98.66, Mn 0.83, Si 0.24, C 0.17, Cu 0.024 and S 0.0093. Several electrodes were elaborated from the original plate sample with a thickness of 18 mm. They were embedded in resin, and the working surface of only 2 cm^2 was exposed. They were polished up to grade 1200 with a series of silicon carbide grit papers, rinsed with distilled water, degreased in acetone and immediately transferred into the test medium. The electrochemical tests were carried out in a conventional three electrodes cell. The cell contained the working electrode, a graphite counter electrode and a saturated calomel reference electrode. The electrochemical measurements were realised using a Voltalab Radiometer Analyser

(PGZ 301), controlled by Volta Master 4 software for both tests: linear polarisations and electrochemical impedance spectroscopy.

Experiments were carried out in two distinct test mediums:

- Natural seawater collected from the port of Algiers (Mediterranean sea) containing Cl$^-$ (20,400 mg l^{-1}), Na$^+$ (11,820 mg l^{-1}), Mg^{2+} (1,010 mg l^{-1}), Ca^{2+} (394 mg l^{-1}), SO$_4^{2-}$ (1250 mg l^{-1}) and HCO$_3^-$ (219 mg l^{-1}), whereas others species are at lower concentrations. The pH was 8.3.
- Sterile seawater was obtained by sterilising natural seawater at 120 °C and under 1 bar during 20 min [12].

Electrodes were immersed simultaneously in these electrolytes which were frequently renewed up to 30 days. All experiments were performed at room temperature oscillating between 15 °C and 20 °C.

After different exposure times, linear polarisation plots were recorded at a scan rate of 1 mV s^{-1} within the range of −10 to +10 mV versus the open circuit potential (OCP). EIS measurements were performed under OCP using a 10 mV amplitude sinusoidal signal along the frequency range of 10^5 to 10^{-2} Hz. All corrosion experiments: OCP measurements, linear polarisation and impedance plots are realised according to time for monitoring the evolution of the electrochemical characteristics of metal surfaces.

SEM and energy dispersive X-ray spectrometry (EDX) analysis were performed using fresh rust layer samples of about 1 cm^2 area, immersed up to 14 and 30 days in natural seawater and up to 30 days in sterile seawater. When carbon steel is immersed in natural medium, it may form a biofilm on the metal surface. In this case, before the SEM observation, rust samples were washed with sterilised seawater, followed by a pre-treatment of dehydration in a graded ethanol series of 25%, 50%, 75%, 90% and 100% ethanol during 10 min for each. Thereafter, in order to observe metallic surfaces under corrosion products layer, these previously immersed surfaces were chemically cleaned according to the procedure described by the ASTM G1-03 norm [18]. The SEM images were performed using a scan microscope (JEOL ESEM FEG, Philips XL30 model) using backscattered and secondary electrons as well as EDX analysis.

Results and discussions

EIS measurements

EIS is a non-destructive electrochemical technique for characterising electrochemical reactions at the metal/solution interface and corrosion products and biofilms formation [19].

Figures 1 and 2 show the Nyquist and Bode plots, respectively, of carbon steel in natural seawater for different immersion periods. From the Nyquist plots (Fig. 1) and the frequency dependence of the phase angle (Fig. 2b), it can be concluded that only one time constant determines the corrosion reaction at E_{corr} for 0, 7, 18, 21 and 30 days. The corresponding Nyquist plots exhibit semi-circles that are flattened with the centre below the real impedance axis. This behaviour is typical of solid metal electrodes that show a frequency dispersion of the capacitive properties [20]. The diameter of the semi-circle impedance loop corresponds to the charge transfer resistance related to the formation of the corrosion products layer. Between 0 and 7 days, this resistance increases slightly with time. Thereafter, a change in complex plots with a straight line at low frequencies is observed, when the sample is exposed to seawater during 10 and 14 days. The straight line, corresponding to a second time constant, crosses the real axis at an angle smaller than 45°. This behaviour can be attributed to the diffusion process at the electrolyte–electrode interface. The Warburg impedance relevant at small frequencies results in a linear behaviour with a slope of 45° in the Nyquist plot. The magnitude of the Warburg impedance $|Z_w|$ is inversely proportional to the square root of the frequency $(1/(\omega)^{0.5})$, with a slope value of -0.5, according to the so-called "infinite" Warburg impedance equation: $|Z_w| = \sqrt{2}\sigma/\omega^{0.5}$ where σ is the Warburg coefficient. This impedance can be observed when the region available for diffusion is not a limiting one [21].

It should be pointed out that the impedance spectra described above do not always fit real situations. In such cases, when the electrochemical cell is stirred, the diffusion layer becomes finite. Consequently, the "finite" Warburg impedance appears resulting in a linear or bending curve of the impedance towards the real axis at very low frequencies [21]. In this case, Z_d is introduced to explain diffusion behaviour of electrode processes at low frequencies by considering just a finite length diffusion line of electro-active species from the bulk of the solution to the electrode.

In Nyquist plots (Fig. 1), the presence of the Warburg impedance shows that the corrosion products layer formed on the steel surface is modified and it may be attributed to the formation of an unstable layer constituted by a mixture of a biofilm and corrosion products [17, 22, 23].

As reported by Yuan [12], the diffusional impedance is primarily related to the microstructure of the biofilm. Its columnar structure contains more open porosity. These defects can provide efficient diffusion channels for reactive species such as oxygen. So, the diffusion process is slow and difficult.

For exposure times longer than 14 days, profiles show capacitive loops. This means that the diffusion process, previously described, does not occur on the electrode. The diameter of these semi-circles undergoes a gradual increase for 18, 21 and 30 days of immersion. This behaviour indicates that the corrosion rate becomes lower at a long exposure time which can be attributed to the formation of a layer with less open porosity.

Figure 3 displays the Nyquist plots of carbon steel in sterile seawater as a function of exposure time at E_{corr}. Two time constants occur for steel in sterile seawater with a deviation from the ideal behaviour (semi-circle with the centre below the axis of the complex impedance plot). A series of two capacitive loops appears at high frequencies (except at the initial time of immersion) and this is due to the conditioning layer formed on the metal surface. According to some authors [12, 17, 22], this layer results from the precipitation of various species like chlorides, phosphates and organic compounds which exists in seawater and forming the outer layer.

The diameter of these high frequency loops remains constant. A second capacitive loop in the EIS Nyquist plan (Fig. 3) or a second time constant in EIS Bode plan (Fig. 4b) appeared at middle frequencies. Their diameter increases with time, implying a decrease in the corrosion

Fig. 1 Nyquist plots of BV-grade A carbon steel in natural seawater for different exposure times
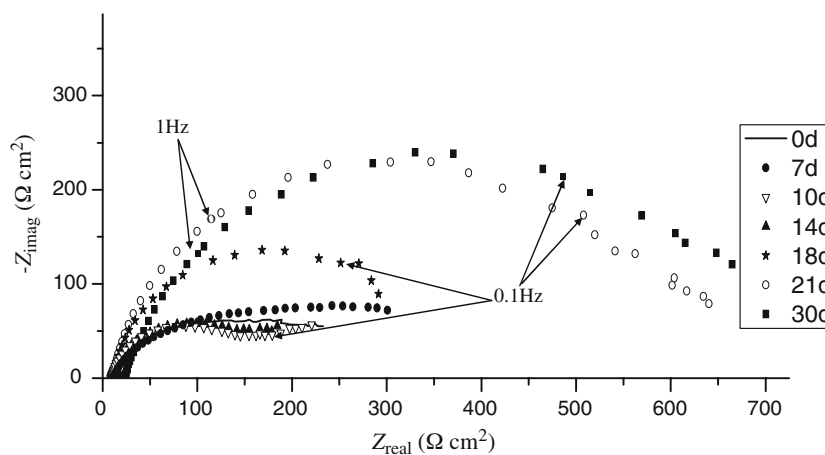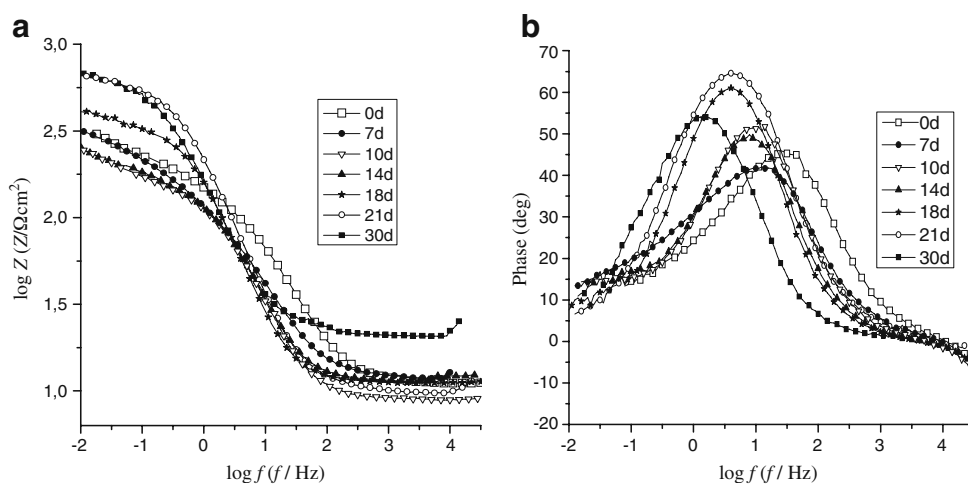
rate of carbon steel at a longer exposure time. The medium frequency response is commonly attributed to the charge transfer reaction with a formation of a corrosion products layer. Bode magnitude plots with respect to Fig. 4a show that the total impedance magnitudes of the sample at the lowest frequencies increased with exposure time, indicating that the increase in the corrosion resistance is due to the formation of a protective oxide layer as previously shown. From the respective bode phase angle plots (Fig. 4b), two peaks (maxima) can be distinguished. The high frequencies peak is not clearly observed but displaces slightly that of middle frequencies to the lower scale.

The phase angle magnitude corresponding to the middle frequencies peak (Fig. 4b) increases with time involving a decrease of the corrosion rate. This indicates the evolution of the corrosion products thickness or a dielectrics modification caused by a change in the physical nature (good compactness) of the latter [17, 19, 24].

While carrying out the impedance study, it was found that there are two time constants when steel is immersed in sterile seawater (except at initial time) but only one time constant if steel is immersed in natural seawater over 0, 7,

18, 21 and 30 days. In this last medium, the diffusion process attributed to the presence of a natural biofilm for 10 and 14 days of immersion time involves two time constants.

The electrical circuits used to describe carbon steel exposed to both conditions taking into account the contribution of each phenomenon, i. e. film formation and oxygen diffusion, are represented in Fig. 5. These circuits have been previously proposed for studying the steel corrosion process in environments containing biological species [13, 22, 23]. Figure 5a illustrates the equivalent circuit $R(QR)$ corresponding to a single layer of corrosion products for steel in natural seawater without diffusional process contribution. Figure 5b shows the equivalent circuit $R(Q(RZ_d))$ for a single layer in which a finite Warburg element was included, describing the diffusional process influenced by the biofilm corresponding to 10 and 14 days of immersion times. The equivalent circuit $R(Q(R(QR)))$ of a bi-layer for a sterile medium, when an outer layer of organic/inorganic compounds and an inner layer of corrosion products are formed, is illustrated in Fig. 5c.

The electric elements of the equivalent circuits of Fig. 5 can be associated, in this way: R_e is the electrolyte solution
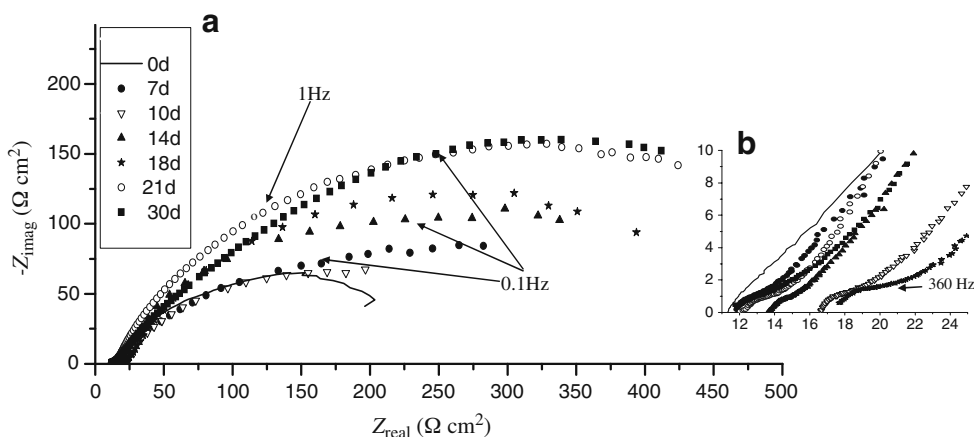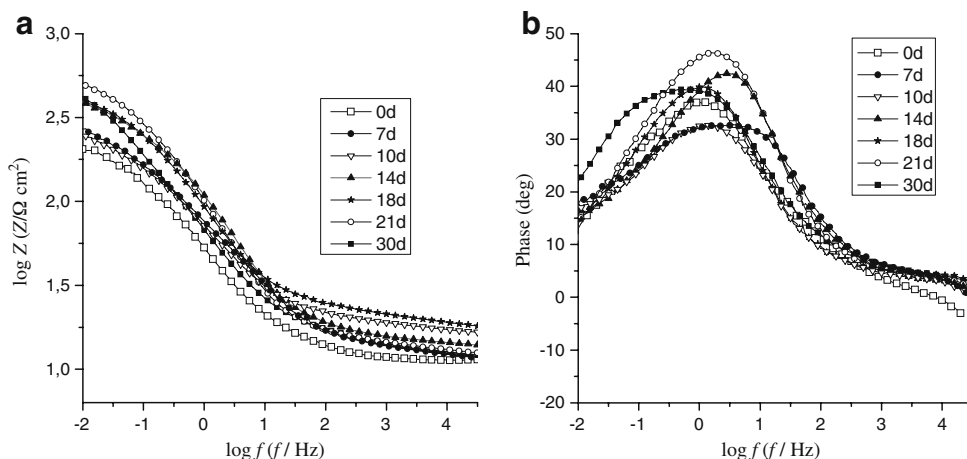
resistance, R_{ct} is the resistance associated with the charge transfer process occurring at the interface between the metal and the corrosion products. Q_{ct} is the non-ideal double layer capacitance used in order to consider the roughness of the interface. R_{mix} and Q_{mix} are the parameters used to imply that a heterogeneous biofilm is dispersed through corrosion products which constitute a mixture layer. A finite Warburg element, Z_d, is an electrical arrangement related to the diffusional process of different species such as oxygen through the biofilm. The terms Q_0 and R_0 are the parameters related to the outer layer of organic/inorganic compounds formed at the interface in sterile seawater.

The observed plots show semi-circles with the centre below the x-axis. These depressed semi-circles can be explained by the heterogeneous nature of the solid surface or by the dispersion of some physical properties values of the system [19, 20]. Consequently, the layer at the interface cannot be considered as an ideal capacitor and the constant phase element (CPE) is often used as a substitute for the ideal capacitor. Therefore, the relevant impedance Z_{CPE} is defined as [25]:

$$Z_{CPE} = \frac{1}{Q(j\omega)^n} \tag{1}$$

Where Q is the CPE constant (Ω^{-1} cm^{-2} s^n) and $j^2 = -1$. For $n = 1$, the CPE can be identified as a capacitance. n, the CPE exponent, is such that $0 \leq n \leq 1$. The plot of the imaginary part of the impedance as a function of frequency gives a straight line with a slope equal to n [26]. ω is the circular frequency. Since $n < 1$, the capacitance can be calculated

Fig. 5 The equivalent circuits diagrams used for the modelling of the impedance spectra for the BV-grade A naval steel based on **a** single-layer model, **b** single-layer Warburg model and **c** bi-layer model
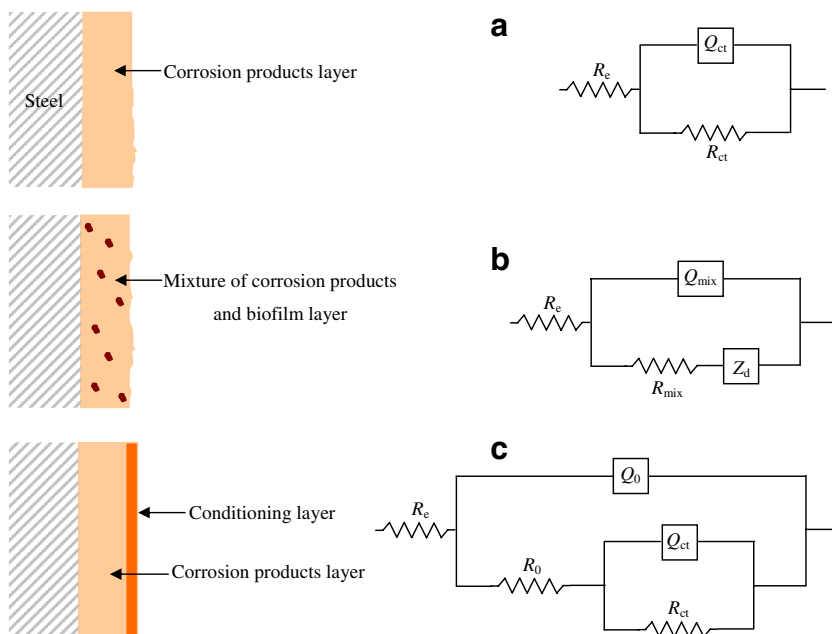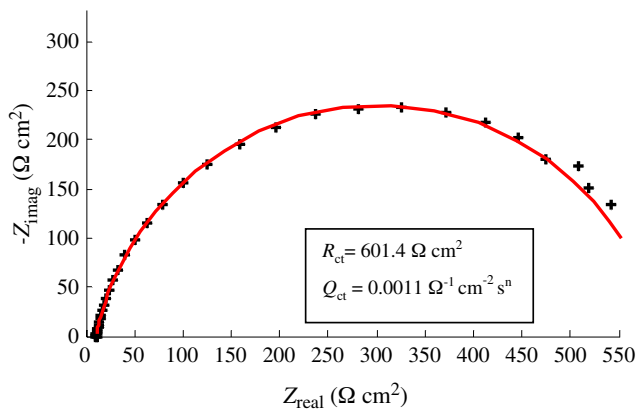
Fig. 6 Nyquist impedance spectra obtained in natural seawater for 21 days of immersion: *solid line* represents fitted curve according to the model proposed on Fig. 5a

from the CPE parameters determined experimentally using the following equation according to Boukamp [27]:

$$C_{eq} = (QR_{ct})^{1/n}/R_{ct} \qquad (2)$$

where R_{ct} is the charge transfer resistance.

For the equivalent circuit showed in Fig. 5a, the total impedance can be formulated as:

$$Z_{eq}(\omega) = R_e + \frac{R_{ct}(1 + A\,R_{ct}\,Q_{ct}\,\omega^n)}{(1 + A\,R_{ct}\,Q_{ct}\,\omega^n)^2 + (B\,R_{ct}\,Q_{ct}\,\omega^n)^2}$$
$$- j\frac{B\,R_{ct}^2\,Q_{ct}\,\omega^n}{(1 + A\,R_{ct}\,Q_{ct}\,\omega^n)^2 + (B\,R_{ct}\,Q_{ct}\,\omega^n)^2} \qquad (3)$$

where R_e is the electrolyte resistance. The asymptotic limit of the real part of the impedance for the circuits shown in Fig. 5 is R_e at high frequencies. This value is most easily obtained.

A and B are the real and the imaginary parts of j^n, respectively, R_{ct} is the charge transfer resistance, Q_{ct} is the CPE related to the charge transfer reaction. The impedance spectra obtained in natural seawater, after different exposure periods and in the absence of the mass transport processes, are analysed and fitted according to this circuit. As an example, Fig. 6 displays the experimental and fitted Nyquist plots obtained for carbon steel immersed in this medium over 21 days.

When the biological effect predominates, which corresponds to 10 and 14 days of immersion in natural seawater, Warburg impedance is exhibited to represent the finite length diffusion and the equivalent circuit illustrated in Fig. 5b is assumed. A constant phase element (Q_{mix}) justifying a layer of corrosion products in the presence of an adherent biofilm is associated to this behaviour. According to this circuit, the total impedance is:

$$Z_{eq}(\omega) = R_e + \frac{(R_{mix} + Z_d(\omega))}{1 + (j\omega)^n Q_{mix}(R_{mix} + Z_d(\omega))} \qquad (4)$$

where the convective diffusion impedance $Z_d(\omega)$ can be given for a finite diffusion layer by [28, 29]:

$$Z_d(\omega) = \sigma(\omega)^{-0.5}(1 - j)\tanh\left(\delta\sqrt{\frac{j\omega}{D}}\right) \qquad (5)$$

σ is the Warburg coefficient, δ is the Nernst diffusion layer thickness and D is the average value of the diffusion coefficients of diffusing species. In the fitting process, a cotangent-hyperbolic diffusion admittance Y_d is considered; it can be given by [28]:

$$Y_d = Y_0 \sqrt{j\omega}\coth(\beta\sqrt{j\omega}) \qquad (6)$$

where $\beta = \delta/\sqrt{D}$ and $Y_0 = 1/\sigma\sqrt{2}$. When the β ratio is divided by Y_0, it can give information about the diffusion resistance of a protective film of a finite length [12]. Separating Y_d into real and imaginary parts leads to [28]:

$$Y_d = Y_0 \frac{1}{2}\sqrt{2\omega}\left[\frac{\sinh(\beta\sqrt{2\omega}) + \sin(\beta\sqrt{2\omega})}{\cosh(\beta\sqrt{2\omega}) - \cos(\beta\sqrt{2\omega})} + j\frac{\sinh(\beta\sqrt{2\omega}) - \sin(\beta\sqrt{2\omega})}{\cosh(\beta\sqrt{2\omega}) - \cos(\beta\sqrt{2\omega})}\right] \qquad (7)$$

The real part only of Y_d is used for data fitting to calculate β and Y_0 at low frequencies. Figure 7 shows the measured and fitted plots of this part for natural seawater after an immersion time of 10 days. As it is illustrated, a good agreement has been reached between both plots.

The equivalent circuit given in Fig. 5c exhibits two time constants and illustrates the formation of a conditioning layer of organic and inorganic compounds as well as the activation control processes attributed to the formation of a second layer of corrosion products. In this particular case, the determination of the real and the imaginary parts issued from the total impedance is too complicated when a CPE is considered. For this reason, these parts are evaluated by using an ideal capacitance instead of the CPE.
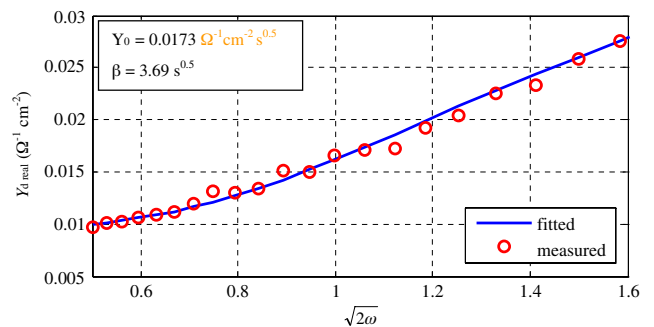

Fig. 7 Real part of diffusion impedance spectra at low frequencies obtained in natural seawater for 10 days: *solid line* represents fitted result according to Eq. 7

The real part of the total impedance can be obtained by standard calculations and is given by the following expression:

$$\text{Real}(Z_{eq}) = R_e + \frac{a + b\,\omega^2}{1 + c\,\omega^2 + d\,\omega^2} \quad (8)$$

Where:

$$a = R_0 + R_{ct}$$

$$b = R_0 \tau_{ct}^2$$

$$c = \tau_0^2 + \tau_{ct}^2 + C_0 R_{ct}(2\tau_0 + C_0 R_{ct} + 2\tau_{ct})$$

$$d = \tau_0^2 \tau_{ct}^2$$

τ_0 and τ_{ct} are time constants of a conditioning layer and a charge transfer process, respectively.

To evaluate the parameters of these circuits, the "curve fitting toolbox" of MATLAB software is used to fit the measured data. The fitting procedure is performed using a non-linear least squares method based on the Levenberg–Marquardt algorithm. Following the data fitting, the success of this procedure is evaluated by controlling the sum of squares due to error (SSE) defined by the following expression:

$$\text{SSE} = \sum_{i=1}^{n} (y_{mi} - y_{fi})^2 \quad (9)$$

Where y_{mi} and y_{fi} are the measured and the fitted data in the curve, respectively.

The main results of the fitting procedure are presented in Tables 1 and 2. During the first 7 days, the charge transfer resistance of carbon steel in natural seawater (Table 1) increases slightly (from 150.2 to 164.3 Ω cm^2) and this is due to the increase in the thickness and/or compactness of the corrosion products layer but, afterwards, decreases from 164.3 to 139.5 Ω cm^2. This result indicates that some bacteria cells have probably colonised on the surface and have formed a biofilm. This phenomenon causes a severe damage such as pitting corrosion accompanied by break-down and a degradation of the protective properties of the film formed, inducing an increase of the active area on the carbon steel surface.

This attack of bacteria can be correlated to the stage of their proliferation. After 14 days of immersion, R_{ct} increases with exposure time due to the formation of a thick protective layer recovering the biofilm. The development of biofilm is a dynamic process. Consequently, the biofilm yields an unstable effect on the capacitance: this electrical magnitude fluctuates consisting on continuous link and growth phase (10 and 14 days), when charge transfer resistance and capacitance decrease related to the growing active area due to the formation of the pores and active sites, then death phase by the coating of the biofilm with a corrosion products layer. That is observed in several investigations performed in medium containing micro-organisms which revealed fluctuations of the capacitance associated with the biofilm formation at the interface [19, 22, 30, 31].

In both natural and sterile seawaters, the oxide layers have a capacitating behaviour deviating from the behaviour of the ideal capacitor ($n<1$). This phenomenon is well-known as the dispersing effect. The frequency dispersion behaviour is probably related to the inherent heterogeneous nature of the solid surface due to the complexity of the

Table 1 Fitting parameters of impedance spectra of BV-grade A carbon steel in natural seawater after various immersion times

| Time (days)	0	7	10	14	18	21	30
Equivalent circuit	R(QR)		R(Q(RZ$_d$))		R(QR)		
R_e (Ω cm^2)	10.91	11.59	8.94	11.48	11.1	9.9	21.78
Q_{ct} (Ω^{-1} cm^{-2} s^n)	0.00048	0.00220	–	–	0.00101	0.00110	0.00122
R_{ct} (Ω cm^2)	150.2	164.3	–	–	355.2	601.4	610.8
n	0.79	0.73	0.82	0.83	0.85	0.83	0.84
R_{mix} (Ω cm^2)	–	–	139.5	144.1	–	–	–
Q_{mix} (Ω^{-1} cm^{-2} s^n)	–	–	0.00133	0.00126	–	–	–
Y_0 (Ω^{-1} cm^{-2} s$^{0.5}$)	–	0.0173	0.0158	–	–	–	–
β (s$^{0.5}$)	–	–	3.69	2.51	–	–	–
σ (Ω cm^2 s$^{-0.5}$)	–	–	40.73	44.81	–	–	–
C_{eq} (μF cm^{-2})	238.58	1,509.96	918.88	888.39	842.86	1,010.73	1,153.52
τ (s)	0.035	0.248	0.128	0.128	0.299	0.607	0.704
SSE	8.2 10^{-3}	5.8 10^{-3}	1.7 10^{-5}	9.2 10^{-5}	3.4 10^{-3}	2.6 10^{-3}	3.1 10^{-3}

Table 2 Fitting parameters of impedance spectra of BV-grade A carbon steel in sterile seawater after various immersion times

Time (days)	0	7	10	14	18	21	30
Equivalent circuit	$R(QR)$	$R(Q(R(QR)))$					
R_e (Ω cm^2)	11.77	11.79	16.61	13.72	17.40	12.22	11.71
C_0 (μF cm^{-2})	–	14.28	17.25	12.73	6.01	14.45	15.45
R_0 (Ω cm^2)	–	2.45	3.42	2.71	4.34	3.30	3.41
τ_0 (s) 10^{-5}	–	3.5	5.9	3.45	2.61	4.77	0.53
n_0	–	0.94	0.90	0.90	0.90	0.90	0.91
C_{ct} (μF cm^{-2})	6,430	7,310	6,380	2,530	4,300	3,920	880
R_{ct} (Ω cm^2)	173.1	306.9	298.1	339.9	453.6	577.2	689.3
τ_{ct} (s)	1.11	2.24	1.58	0.86	1.97	2.26	0.61
n_{ct}	0.58	0.58	0.56	0.62	0.62	0.67	0.57
SSE	$8.9 \ 10^{-2}$	$1.2 \ 10^{-1}$	$1.3 \ 10^{-1}$	$2.2 \ 10^{-1}$	$6.1 \ 10^{-2}$	$6.2 \ 10^{-2}$	$9.1 \ 10^{-2}$

seawater composition [23]. In sterile seawater, this parameter is smaller than that observed in natural seawater. Indeed, the porous and non-protective conditioning layer adheres strongly to the underlying oxide layer and probably contributes to the complexity of surface conditions [32].

For the samples immersed in sterile seawater, the variation of R_0 and C_0, representative of a charge transfer resistance and capacitance of conditioning layer, respectively, is small and relatively unchanged for all the exposure periods indicating thus a stability and homogeneous distribution of this layer. On the contrary, the charge transfer resistance R_{ct} of the inner layer increases continuously along 30 days and it is close to that of the corresponding sample in natural seawater at a longer immersion time.

Capacitance's magnitude generally decreased with time, indicating that corrosion products become low electric conductor and usually less porous. Passive layer formed by corrosion products has acquired more protective properties in the absence of micro-organisms in seawater.
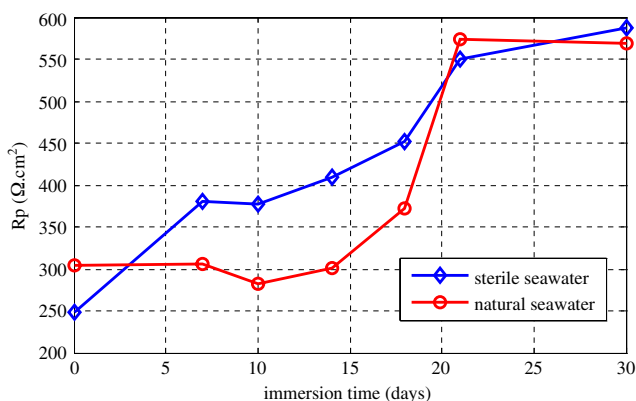
Fig. 8 Polarisation resistance determined from linear polarisation of carbon steel in natural and sterile seawaters

Linear polarisation

Linear polarisation measurements can be used to calculate corrosion parameters such as the polarisation resistance and/or the corrosion current density according to Stern and Geary's law when the cathodic and anodic Tafel slopes are determined from Tafel plots [33]. Figure 8 shows the evolution of the polarisation resistance (R_p) of the carbon steel in natural and sterile mediums. There is a good concordance between these results and those obtained by EIS method. In natural seawater, the polarisation resistance remains constant within the first 7 days, then, it decreases slightly up to 14 days. This result is consistent with the presence of a biofilm having a certain ability to accelerate the corrosion process and to decrease the polarisation resistance up to immersion times of 10 and 14 days. Furthermore, R_p increases again. In sterile seawater, this resistance increases generally with time indicating that a stable layer of oxides protects the metal from corrosion. Probably, its thickness increases with the increasing of the immersion time.

SEM analysis

The obtained SEM micrographs of carbon steel surface immersed for 14 and 30 days in natural seawater are shown in Figs. 9 and 10, respectively. It should be noted that the picture of Fig. 9 is obtained using backscattered electrons, whereas the pictures of Fig. 10 are obtained using secondary electrons.

As it can be shown in Fig. 9, a biofilm is developed on the carbon steel surface after 14 days of immersion in natural environment. Dense bacterial cells sharing the space with extracellular polymeric substances are localised as tubercles dispersed through corrosion products. These aggregates with a diameter reaching about 15 μm constitute
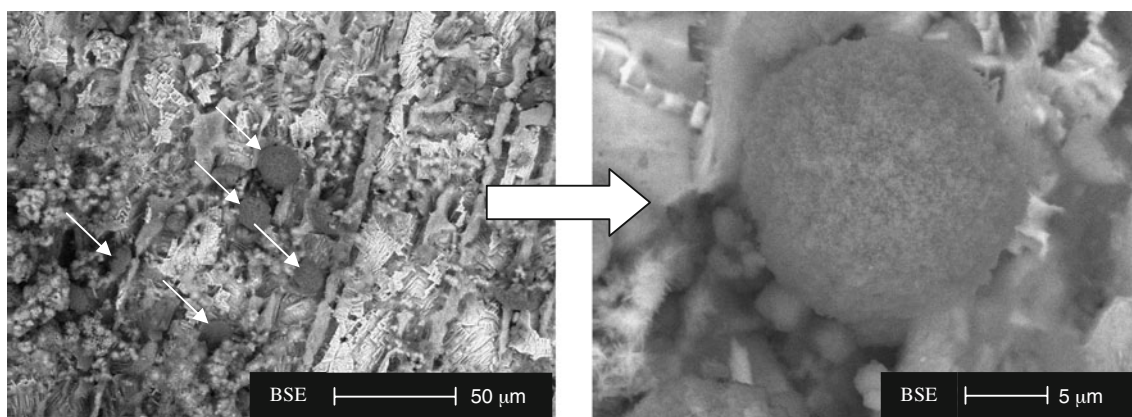
Fig. 9 SEM images of BV-grade A naval steel in natural seawater immersed for 14 days: heterogeneous biofilm formed on the surface

a barrier for the diffusion of active species such as oxygen and chlorides, giving rise to local gradients which can provide physicochemical conditions at the localised sites to initiate a pitting corrosion [34]. For a longer immersion time, the SEM images of the metallic surface immersed for 30 days show corrosion products with a globular morphology on the entire surface, as illustrated in Fig. 10a. In order to observe the lower part of the film, an artificial defect

through a scarification using a cutter blade was made as shown in Fig. 10b.

The corrosion products can be divided into three layers: an outer layer with globular and cluster morphology. It may be a contribution of goethite (α-FeOOH) together with a lepidocrocite (γ-FeOOH) iron hydroxides according to previously observations [13, 35, 36]. Furthermore, in contact with some bacteria such as iron-reducing bacteria
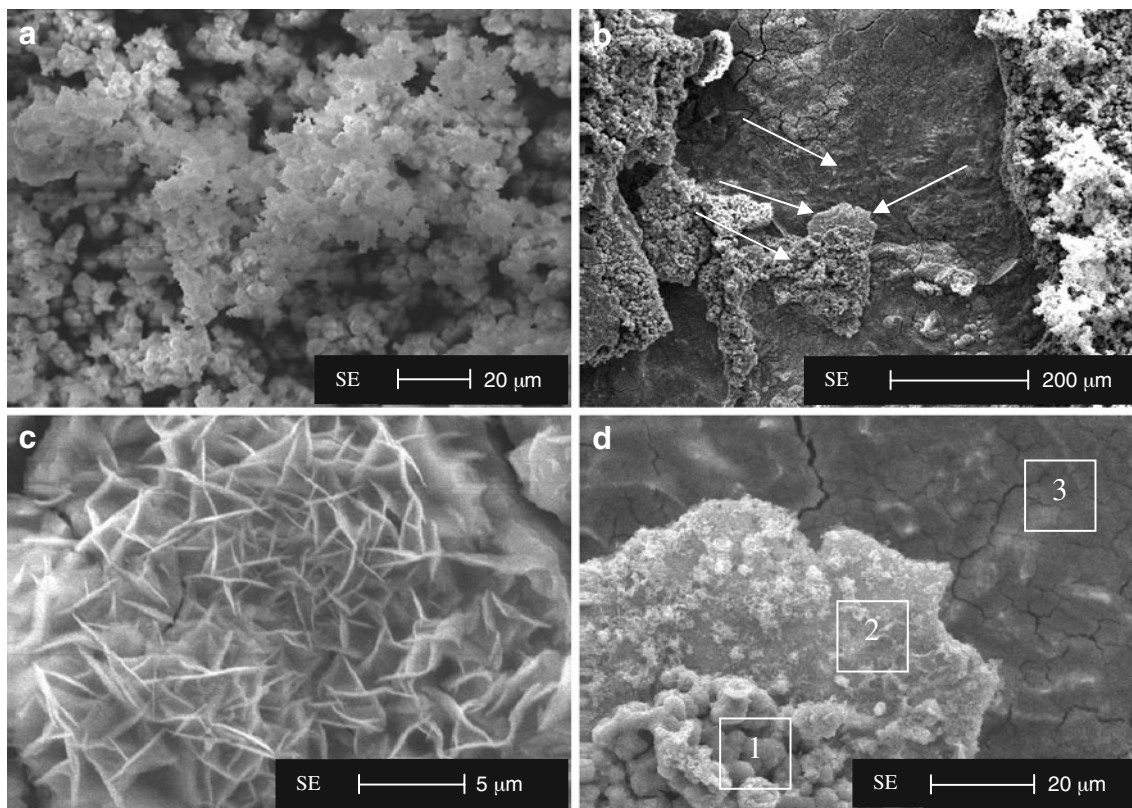

Fig. 10 SEM images of BV-grade A naval steel in natural seawater immersed for 30 days: a globular morphology on the whole of the outer surface, b the artificial defect carried out on the surface showing corrosion products divided into three layers indicated with *arrows* pointing right, c laminar structure of some inner layer, d magnification of the region of (b) showed by the *arrow* pointing *left*

Element	Fe	O	Cl	Mg	Ca	S	Si
Atomic%	46.03	48.39	2.60	1.91	0.38	0.38	0.31

Region 1

Element	Fe	O	Cl	Mg	Na	C
Atomic%	28.71	63.01	0.73	2.21	4.02	1.32

Region 2

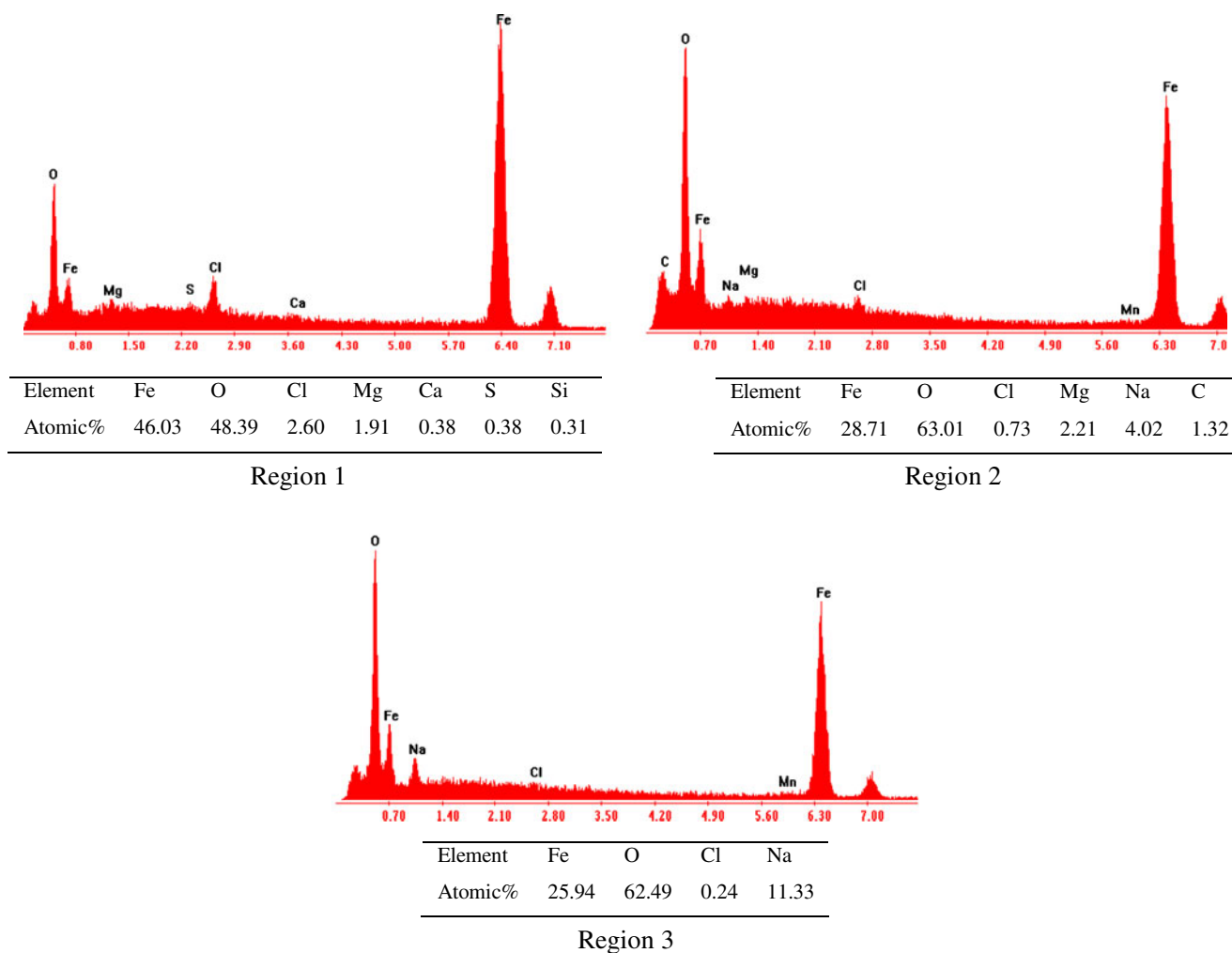| Element	Fe	O	Cl	Na
Atomic%	25.94	62.49	0.24	11.33

Region 3

Fig. 11 EDX spectra of carbon steel coupon in natural seawater after an immersion time of 30 days corresponding to *rectangular areas* on the three layers showed in SEM image Fig. 10d

in seawater, further oxidation of Fe(II) to Fe(III) occurred in the outer part of the corrosion products with a precipitation of solid ferric hydroxide Fe(OH)$_3$. This hydroxide can undergo dehydration giving rise to ferric hydroxides FeOOH. It appeared that this layer was porous, easily peeled off from the carbon steel surface and provided a slight or no protection to the substrate [36].

The EDX spectra were performed on different sites characteristics of representative 30 days sample to evaluate the chemical composition of corrosion products on the steel surface. The EDX analysis shows that the main elements are Fe and O. Other minor elements are present, namely Na, Cl, Mg, S, Si and Ca. They probably arise from seawater. It can be seen that chloride is mainly present in the outer part of the rust layer. The outer part is loose and very porous, and pores were filled with seawater. In contrast, the inner part contains much less chloride (region3). The elemental peak intensities are different. When shifting from the outer towards the inner layer in natural seawater, Fig. 11 shows
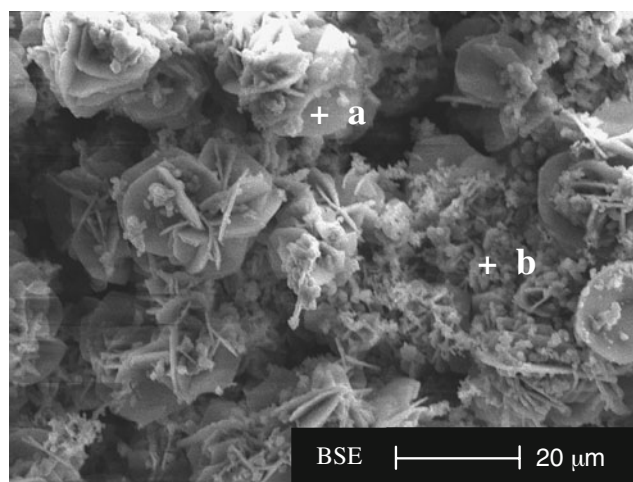

Fig. 12 SEM images of BV-grade A naval steel immersed for 30 days in sterile seawater

Element	Fe	O	Cl	Si
Atomic%	25.11	74.21	0.46	0.22

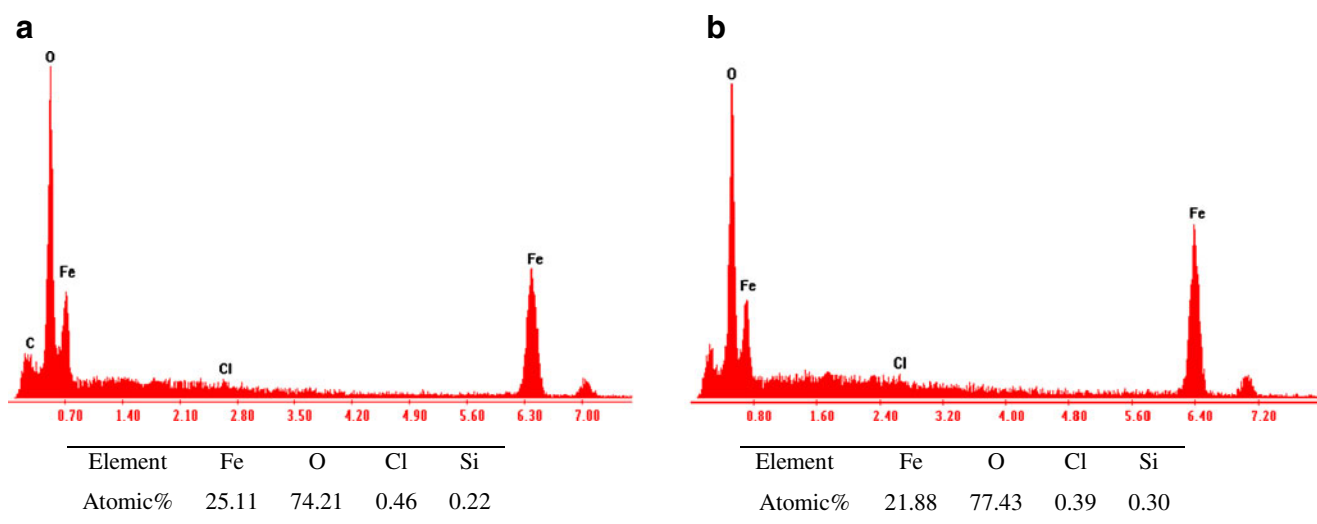| Element	Fe	O	Cl	Si
Atomic%	21.88	77.43	0.39	0.30

Fig. 13 EDX spectra of carbon steel sample in sterile seawater after an immersion time of 30 days corresponding to locations along the various structures showed in SEM image Fig. 12

that the amount of iron has decreased till about 44% and chlorine 91%. Inversely, the amount of oxygen has increased to about 29%.

The large amount of iron and chlorine in the outer layer is justified by the effect of bacteria cells inducing further oxidation from Fe(II) to Fe(III) probably with a formation of soluble Fe(III) complexes and a subsequent precipitation of solid ferric hydroxide Fe(OH)3 as previously said, the occurring of the latter being helped by the presence of chlorine in the corrosive medium [37].

The inner (region3) and the middle (region2) layers have a platelet structure enclosing more oxygen and carbon as shown in Fig. 11. These rust layers can include $FeCO_3$ protective film whose precipitation could be favoured by an increase of ferrous ion concentration [38].

In sterile seawater, the outer layer is different from that observed in the case of natural seawater. Figure 12,

obtained using backscattered electrons, exhibits corrosion products coexisting partly as crystalline and partly as amorphous structures. EDX spectra analysis (Fig. 13) shows that the Fe peaks are considerably reduced relatively to the sample immersed in natural seawater. The reduction of the Fe peaks suggests probably that the surface is well protected and the metal dissolution is slowed down. This statement can be justified by the fact that this outer layer contains less chloride comparatively to the case of natural seawater. Thus, the layer may be less porous and then more protective.

Optic microscope analysis

Figure 14 displays carbon steel surfaces exposed in natural and sterile seawater, respectively, after removal of rust layers by chemical cleaning. Black spots illustrated in
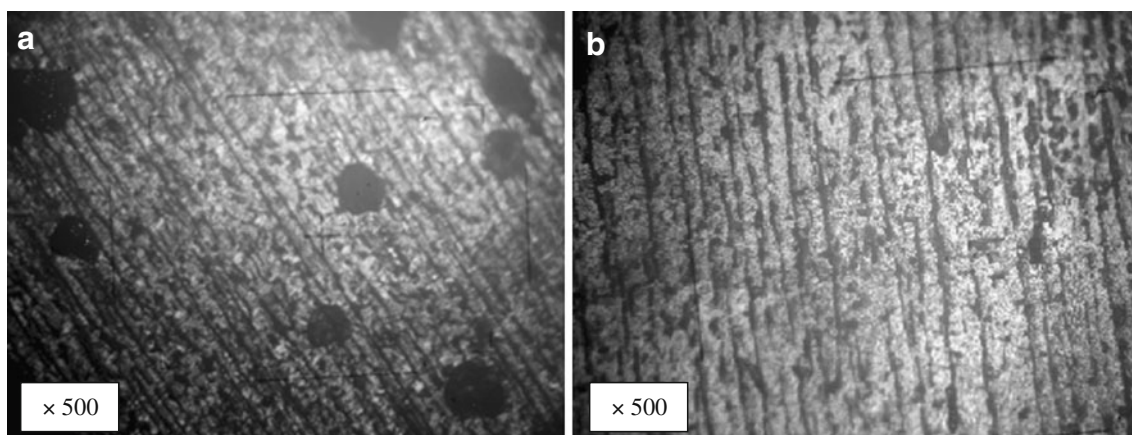

Fig. 14 Optic microscope images of the corroded surfaces after removal of the corrosion products layer after an immersion time of 30 days in: **a** natural seawater, **b** sterile seawater

Fig. 14a show the impact of the localised tubercles of bacteria and theirs extracellular polymeric substances as well as the presence of the aggressive chloride ions (Cl^-) at the interface in natural seawater.

These spots represent deep pits. Contrarily, the surface immersed in sterile seawater presented in Fig. 14b exhibits no or slight pits which can be the result of the localised corrosion caused by chloride and sulphide ions within the same immersion time.

Conclusion

Comparative studies have been carried out on the BV-grade A naval carbon steel under two experimental conditions: natural seawater and sterile seawater using electrochemical impedance spectroscopy and linear polarisation techniques. The principal results can be summarised as follows:

- Complex impedance plots exhibit one and two deformed capacitating semi-circles in natural and sterile seawater, respectively. In natural medium, the semi-circle is accompanied by a straight line characteristic of mass transport process after 10 and 14 days of immersion times.
- A biofilm, typical of a natural environment, mixed to a corrosion products layer is formed after a period of immersion of 10 days. This mixture affects the corrosion behaviour of carbon steel subject to mass transport limitation process. Both electrochemical techniques (EIS and linear polarisation) have shown that this biofilm produces a decrease in charge transfer and polarisation resistances.

Beyond 14 days, carbon steel became more resistant to corrosion. This favourable behaviour can be related to the oxide layer formed by precipitation reactions increasing thus its thickness or improving its physical properties such as compactness and adherence. Consequently, the charge transfer and polarisation resistances increase at the same time.

- In sterile seawater, two layers are formed. A non-protective outer layer due to the chemical precipitation of organic or inorganic species present in seawater covering an inner layer composed essentially by oxide products. In this case, the evolution of the protective properties of corrosion products layer is proportional to the exposure time because the charge transfer and polarisation resistances increase and capacitance values decrease with time.
- SEM images reproduced from carbon steel surface after 14 days of immersion in natural medium revealed the non-uniform dispersion of the localised tubercles of the biofilm. The micrographs of the chemically cleaned

surface exhibited a great number of micro-pits scattered on the whole surface with comparison to the surface immersed in sterile seawater where no or just a few shallow pits were observed for the same immersion period.

It can therefore be concluded that both bacterial colonisation and aggressive chloride ions (Cl^-) play significant roles in the initiation and propagation of pitting corrosion.

SEM images showed also that the corrosion products layer sampled from carbon steel immersed in seawater for 30 days can be divided roughly into three layers. EDX analysis indicates that the outer layer formed on the metallic surface in natural seawater is porous and contains chloride ions and iron. Whereas in sterile seawater, the outer layer contains more oxygen but less iron and chloride ions. This is to suggest that, in the sterile environment, the corrosion products layer was more compact. But this compactness does not improve significantly the corrosion resistance of steel in the sterile environment because the resistance of charge transfer R_{ct} and that of polarisation R_p are close to those obtained in natural environment for longer immersion times.

References

1. Gonzalez JEG, Santana FJH, Mirza-Rosca JC (1998) Corros Sci 40:2141
2. Vandecasteel JP (2008) Petroleum microbiology. Technip Edition, Paris
3. Miečinskas P, Leinartas K, Uksienė V, Juzeliūnas E (2007) J Solid State Electrochem 11:909
4. Marchal R (1999) Oil Sci Technol Rev IFP 54:649
5. Heydorn A, Ersboll B, Hentzer M (2000) Microbiol 146:2409
6. Videla HA, de Mele MFL, Brankevich G (1988) Corros 44:423
7. Mehanna M, Basseguy R, Delia ML, Bergel A (2009) Electrochem Commun 11:568
8. Lovley DR (1991) Microbiol Rev 55:259
9. Franklin MJ, White DC, Isaacs HS (1991) Corros Sci 32:945
10. Moreno DA, Ibars JR, Beech IB, Gaylarde CC (1993) Biofouling 7:129
11. Videla HA (1994) Int Biodeterior Biodegrad 34:245
12. Yuan SJ, Pehkonen SO, Ting YP, Kang ET, Neoh KG (2008) Industrial Eng Chem Res 47:3008
13. Duan J, Wu S, Zhang X (2008) Electrochim Acta 54:22
14. Duan J, Hou BR, Yu ZG (2005) Proc 16th Int Corros Congr Beijing, China
15. Beech IB (2003) Microbiol Today 30:115
16. Liu H, Xu L, Zeng J (2000) Br Corros J 35:131
17. Sosa E, Garcia-Arriaga V, Castaneda H (2006) Electrochim Acta 51:1855
18. ASTM G1-03 Norm. Standard practice of preparing, cleaning, and evaluating corrosion test specimens, Book of standards Volume: 03.02, ASTM International, 2003
19. Yuan SJ, Choong AMF, Pehkonen SO (2007) Corros Sci 49:4352
20. Xu XJ, Ma HY, Chen SH, Xu ZY, Su AF (1999) J Electrochem Soc 146:847

21. Renneberg R, Lisdat F (2008) Biosensing for the 21st century. Springer-Verlag, Berlin Heilderberg, p 199
22. Castaneda H, Benetton XD (2008) Corros Sci 50:1169
23. Santana Rodriguez JJ, Santana Hernandez FJ (2006) Corros Sci 48:1265
24. Bonnel Dabosi AF, Deslouis C, Duprat M, Keddam M, Tribollet B (1983) J Electrochem Soc 130:753
25. Zoltowski P (1998) J Electroanal Chem 1:149
26. Devos O, Gabrielli C, Tribollet B (2006) Electrochim Acta 51:1413
27. Bouckamp BA (1993) Users Man Equivalent circuit ver 4.51, Fac of chem Tech, Univ of Twente, The Netherlands
28. Boukamp BA (1989) Users Man Equivalent circuit, Univ of Twente p 12
29. Yu Z, Pehkonen SO (2004) Water Sci Technol 49:73
30. Monfort MN (2001) Thèse de Doctorat, Université Paris VI, Spécialité: Electrochimie
31. Hilbert LR (2000) PhD Thesis, Technical University of Denmark
32. Yuan SJ, Pehkonen SO (2007) Colloids Surf 59:87
33. Stern M, Geary AL (1957) J Electrochem Soc 104:56
34. Hakkarainen TJ (2003) Mater Corros 54:503
35. Misawa T, Hashimoto K, Shimodaira S (1974) Corros Sci 14:131
36. Kui X, Chao D (2008) Iron Steel Res 15:42
37. Carbucicchio M, Ciprian R, Ospitali F, Palombarini G (2008) Corros Sci 50:2605
38. Dugstad A, Hemmer H (2000) proc NACE corros 2000 (paper No. 24)